Terphenyl(bisamino)phosphines: Electron-rich Ligands for Gold-Catalysis.

Jan-Erik Siewert,[a] André Schumann,[a] Malte Fischer,[a] Christoph Schmidt,[a] Christian Hering-Junghans*[a]

[a] Leibniz-Institut für Katalyse e.V. Rostock, Albert-Einstein-Straße 29a, 18059 Rostock, Germany.

Abstract:

Terphenyl(bisamino)phosphines have been identified as effective ligands in cationic gold(I) complexes for the hydroamination of acetylenes. These systems are related to Buchwald phosphines and their steric properties have been evaluated. Effective hydroamination was noted even at low catalyst loadings and a series of cationic gold(I) complexes has been structurally characterized clearly indicating stabilizing effects through gold-arene interactions.

Introduction

Transition metal catalysis is governed by the influence of multiple factors; however, most crucial are the following three: Metals, substrates and ligands.[1] Among the plethora of ligands used in transition metal catalysis phosphines have been demonstrated to be an invaluable ligand class in a variety of transformations. Buchwald and co-workers have developed the so-called Buchwald-type phosphines, which have been shown to occupy two coordination sites in low-valent Pd-complexes (Figure 1, A).[2-4] In addition to the P-Pd interaction an η^1-Pd–C_{ipso} bonding interaction was found in the complex LPd(dba) (L = 2-(2′,6′-dimethoxybiphenyl)dicyclohexylphosphine; dba = dibenzylidene-acetone).[5] The 2-biphenyl moiety in this ligand class has allowed to achieve the challenging coupling of aryl chlorides and extremely hindered aryl boronic acids in Suzuki-Miyaura cross-coupling reactions. Since their initial synthesis various Buchwald-type phosphines have been presented and are now commercially available (e.g. JohnPhos).[6]

In order to access the electronic properties of phosphines usually Tolman's cone angle and/or electronic parameter (TPE) are utilized, allowing to measure direct ligand metal interactions.[7, 8] In contrast to Pd-catalysis (with mostly square planar complexes), in gold(I)-catalysis the linear coordination mode at gold is operational. This forces substrates into trans- position of the ligand, which enhances its electronic effects. Cationic gold complexes are well suited for the electrophilic activation of alkynes and their subsequent functionalization with a variety of nucleophiles.[9-11] This preference for alkyne activation has been attributed to the low LUMO energies of Au-alkyne complexes, rendering them more electrophilic.[12, 13]

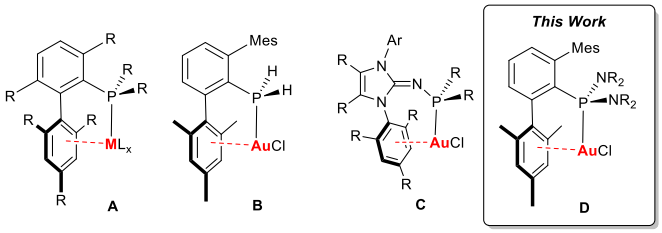

Figure 1. General metal complexes with Buchwald-type ligands (A), related gold complexes from the literature (B, C), and synthetic targets of this study (D).

In Au(I) catalysis a major drawback is the decay of the gold catalyst, which results from reduction of the cationic gold center to gold(0).[14] It has been shown that in many of these transformations electron-rich phosphine ligands outperform their electron-deficient counterparts. For the intermolecular amination of alkynes electron-rich phosphines with a 2-biphenyl moiety are considered superior.[15] Comparing the TEP-values of common Buchwald-type phosphines shows that they do not exceed the donor strength of simple $^tBu_3P$,[8] and the prominent class of N-heterocyclic carbenes (NHCs) are stronger σ donor ligands (Figure 1).[16] Dielmann and co-workers, as well as Sundermayer et al. have recently pushed the electron-donating ability of phosphines beyond their classical endpoint through P-substitution with N-heterocyclic imines (NHIs)[17] or phosphazenes,[18] respectively. In addition, the NHI-functionalization allows the metal center to engage in additional interaction with the aryl-substituents in the N_{NHC}-position of the carbene (Figure 1, C).

Terphenyl-groups, of the general formula 2,6-Ar_2-C_6H_3, have played a leading role in advancing the chemistry of low-valent main group and transition metal species.[19-23] A reagent commonly used to introduce the terphenyl moiety is Ter-Li (Ter = 2,6-Mes_2-C_6H_3),[24] which can be treated with element halides to access Ter-EX_n species.[17, 25, 26] In our hands treatment of Ter-Li with PCl_3 often resulted in trace amounts of Ter-H contaminating the desired Ter-PCl_2 product.[27] Thus, we were interested in a way to circumvent the formation of Ter-H. Ragogna et al. have recently described the successful preparation of $[TerPS]_2$, a source of monomeric phosphinidine sulfides.[28] $[TerPS]_2$ is synthesized by treating Ter-PCl_2 with $S(SiMe_3)_2$. In their study the authors outlined an alternative route towards Ter-PCl_2. Additionally, $TerPH_2$ was shown to form AuCl complexes in which stabilizing arene-interactions with one of the flanking mesityl group are detected (Figure 1, B).[29]

In this contribution we describe the application of the $TerPCl_2$ precursors $TerP(NR_2)_2$ [R = Me (**1Me**), Et (**1Et)**] as Buchwald-type phosphine ligands in gold(I)-catalyzed hydroamination reactions of terminal alkynes (Figure 1, D). The effect of the amino groups was investigated on a theoretical basis and an efficient tool for the estimation of the TEP_{Ni}-value is presented.

Results and discussion

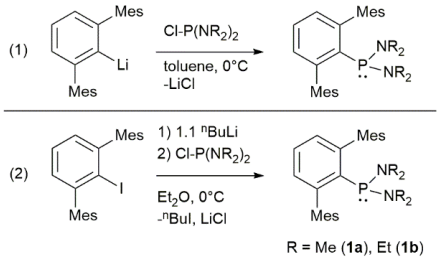

Scheme 1. Two synthetic routes towards terphenyl-substituted bisaminophoshines **1a** (R = Me) and **1b** (R = Et).

Ragogna and co-workers have recently described a route towards $Ter\text{-}PCl_2$ through aminolysis of $Ter\text{-}P(NEt_2)_2$ with dry HCl.[28, 30] Consequently, we prepared $Ter\text{-}P(NR_2)_2$ [R = Me (**1a**), Et (**1b**)] by treatment of isolated Ter-Li with $ClP(NR_2)_2$ (R = Me, Et; an HCl-free P-source) in toluene at ambient temperature (Scheme 1, reaction 1). In case of **1a**, filtration over a celite-padded frit and removal of the solvent resulted in the isolation of an analytically pure colourless solid in 67% yield. For **1b**, after stirring for 1.5 h, the solvent was removed and the residue was extracted with *n*-hexane, concentrated to incipient crystallization and standing at 5 °C overnight afforded **1b** as an analytically pure colourless crystalline solid, in a moderate yield of 40%. We found that consistently higher yields are obtained by starting from Ter-I. Lithiation of Ter-I with 2.5 M ^{n}BuLi (in *n*-hexane) in Et_2O at 0°C and subsequent treatment with $ClP(NR_2)_2$ afforded **1a** (79 %) and **1b** (89 %) in good isolated yields (Scheme 1, reaction 2). In addition, this synthetic approach can be easily scaled and **1b** was prepared on a multigram scale.

Ligands **1a** and **1b** are characterized by ^{31}P NMR signals at 102.5 and 100.2 ppm, respectively, upfield- shifted compared to their respective $ClP(NR_2)_2$ precursors. In the ^{1}H NMR spectrum of **1a** and **1b** two signals for the ortho and para CH_3-groups of the mesityl groups in a 2:1 ratio are observed. In **1a** a doublet corresponding to the two NMe_2 groups is detected, indicating C_2 symmetry in solution. In **1b** a complex multiplet is observed for the methylene protons in the Et-groups of the NEt_2-moiety, and a triplet for the Me-groups. X-ray quality crystals of both **1a** and **1b** were grown from saturated *n*-hexane solutions at 5°C over a period of 24 h and the compounds crystallize solvent-free in the monoclinic space group $P2_1/c$ with four molecules in the unit cell. The phosphorus atoms show a coordination environment deviating significantly from an ideal trigonal pyramid [Σ(<P) (**1a**) 314.03°, (**1b**) 317.26°, cf. $TerPMe_2$[31] 309.0°, $TerPCl_2$[32] 305.58°], which is further supported by NBO analysis [wB97XD/6-31g(d,p) level of theory] showing a 50/50 contribution of 3s and 3p orbitals for the lone pair (LP) on phosphorus.[33] The $P\text{–}C_{Ter}$ bond lengths are [(**1a**) 1.8591(14), (**1b**) 1.813(11) Å] indicative of P–C single bonds [Σr_{cov}(P–C) = 1.85 Å].[34] The P–N distances [(**1a**) P1–N1 1.6981(11) Å, P1–N2 1.6942(12) Å; (**1b**) P1–N1 1.6981(11), P1–N2 1.6942(12); cf. $(Me_3Si)_2NPCl_2$ P–N 1.6468(8) Å][35] are contracted [Σr_{cov}(P–N) = 1.85 Å],[34] hinting at partial double bond character through interaction of the N-LPs with the other σ*(P–N) orbitals as shown through 2nd order perturbation analysis using NBO with stabilization energies for **1a** of 14.5 and 10.2 and for **1b** of 18.1 and 9.5 kcal/mol, respectively. The sum of angles at the N in **1b** deviate from the expected trigonal planar coordination environment, and minimal pyramidalization is observed [Σ(<N1) = 352.78°].

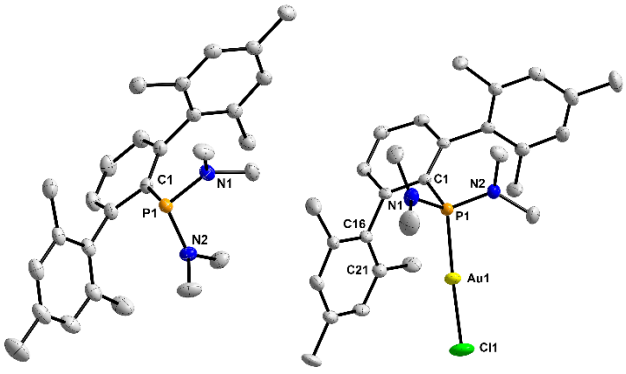

Figure 2. POV-Ray depiction of the molecular structures of **1a** (left) and **2a** (right). Ellipsoids are drawn at 50% probability, 150(2) K. All hydrogen atoms have been omitted for clarity. Selected bond lengths (Å) and angles (°) of **1a** (left): C1–P1 1.8591(14), P1–N1 1.6827(12), P1–N2 1.6850(13), P1–C1 1.8591(14); N2–P1–N1 107.79(6), N1–P1–C1 108.37(6), N2–P1–C1 97.87(6), C25–N1–C26 112.90(13), C25–N1–P1 126.32(11), C26–N1–P1 118.37(11), C27–N2–C28 112.66(13), C27–N2–P1 117.47(10), C28–N2–P1 126.48(10). **2a** (right): P1–N2 1.657(4), P1–N1 1.659(4), P1–C1 1.846(4), P1–Au1 2.2366(11), Cl1–Au1 2.3017(14), C16–Au1 3.2839(33), C21–Au1 3.1008(43); N2–P1–N1 108.5(2), N2–P1–C1 113.3(2), N1–P1–C1 99.33(19); C25–N1–C26 112.1(4), C25–N1–P1 118.2(3), C26–N1–P1 124.0(3), C27–N2–C28 112.5(4), C27–N2–P1 123.4(3), C28–N2–P1 123.5(3); Au1–P1–C1–C2 -128.2(3).

With the structural analysis of **1a** and **1b** in hand the structural resemblence with Buchwald's dialkylbiarylphosphines became evident. These are regarded as privileged ligands in various Pd- and Au-catalyzed reactions. In analogy to the Buchwald systems the 2,6-substitution pattern on the central aryl moiety of the terphenyl-framework, affords a binding pocket about the phosphorus that would allow for arene interactions of a coordinated metal with one of the flanking mesityl groups. Similar systems based on redox-responsive terphenyl-substituted phosphonites have been recently described by Breher and co-workers.[36] In addition, the steric and electronic properties of related $Ar_2C_6H_3$-PR_2 systems have been studied in detail.[37, 38] Combination of **1a** or **1b** with one equivalent AuCl(SMe_2) in CH_2Cl_2 under the exclusion of light at room temperature for 1 h, subsequent concentration and layering with *n*-hexane afforded **2a** (67%) and **2b** (91%) in good to excellent isolated yields as colorless X-ray quality crystals (Scheme 2). Upon coordination the P atom is minimally shielded as shown by a ^{31}P NMR shift of 96.7 ppm (**2a**) and 93.3 ppm (**2b**), respectively. This trend is also reflected in the theoretical NMR shifts obtained from GIAO calculations on the wB97XD/6-31g(d,p)/ECP60MWD level of theory.[33] In the ^{1}H NMR spectrum both complexes show only two signals for the Me-groups of the terphenyl-moiety, indicating free rotation around the P–C_{Ter} axis on the NMR timescale at room temperature. SXRD experiments revealed the expected arene-interactions between the Au(I)-center and one of the ortho-mesityl groups of the terphenyl moiety. **2a** crystallizes in the orthorhombic space group *Pna*2_1 with four molecules in the unit cell, whereas **2b** crystallizes in the monoclinic space group *P*2_1/n with four molecules in the unit cell. Upon coordination to AuCl the sum of angles at phosphorus increases [Σ(<P) (**2a**) 321.13°, (**2b**) 323.55°, cf. (TerPMe_2)AuCl 318.33°][29] and the P–N bonds are contracted by ca. 2% [(**2a**) P1–N1 1.659(4) Å, P1–N2 1.657(4) Å; (**2b**) P1–N1 1.6665(17) Å, P1–N2 1.6604(17) Å] when compared with the free ligands **1a** and **1b**. The complexes show a nearly linear P-Au-Cl arrangement with P–Au distances [(**2a**) P1–Au1 2.2366(11); (**2b**) 2.2445(5) Å; cf. (TerPMe_2)AuCl 2.2964(10) Å][29] in the expected range for phosphine gold complexes.

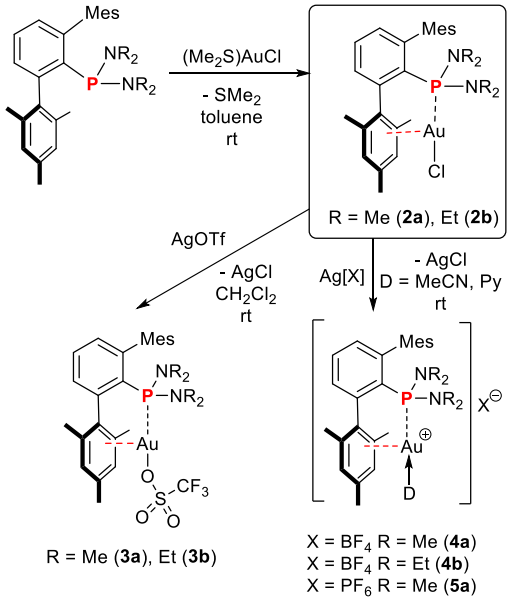

Scheme 2. Synthesis of gold complexes **2** and transformation into **3** and donor-stabilized complexes **4** and **5a**.

In **2a** and **2b** there are close contacts between Au1 and one of the flanking terphenyl groups [(**2a**) C21–Au1 3.1008(43); (**2b**) C17–Au1 2.9707(20) Å], which is in contrast to the known complex (TerPMe_2)AuCl.[29] This stabilizing arene-interaction was further authenticated through an analysis of the electron density of an optimized structure at the wB97XD/6-31g(d,p) level of theory, using the AIM (Atoms in Molecules) approach.[39] This showed a line critical point between Au and C21 (**2a**) and C17 (**2b**) , respectively (see ESI for details).[40]

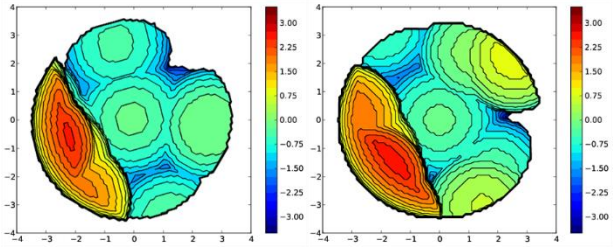

Figure 3. Steric maps of gold complexes **2a** (left) and **2b** (right). Areas in red denote areas of increased bulk, whereas blue is descriptive of less bulk.

Using the SambVca 2.1 online application the steric properties of ligands **1a** and **1b** were analysed (based on the molecular structures of complexes **2**).[41] This showed percent buried volumes (%V_{bur}) of 48.8 % (**1Me**) and 55.4 % (**1Et**), respectively. The %V_{bur} describes how much volume of a sphere centered on the metal [r_{sphere} = 3.5 Å; d_{M-L} = **2a** 2.2366(11); **2b** 2.2445(5) Å] is occupied by the ligand. From the steric maps it is evident that the flanking mesityl group takes up major space in one quadrant of the xy-plane perpendicular to the P–Au-axis (Figure 3), while the NMe_2 groups occupy less space than the NEt_2-groups, which is clearly reflected in the %V_{bur} values. This is in the range of JohnPhos (50.9%), however, exceeds the value of simple phosphines (PPh_3 34.5 %, P^tBu_3 42.4 %).[42]

In a next series of experiments, we investigated the formation of cationic gold complexes. As an entry **2a** and **2b** were treated with AgOTf in benzene and ^{31}P NMR spectroscopy of the reaction mixtures showed the formation of new species with singlet resonance at 86.5 ppm and 78.9 ppm, respectively. Interestingly, the ^{19}F NMR spectrum showed a singlet at −76.6 ppm, which is in agreement with a covalently bound triflate group (c.f. Ter[Me_2(OTf)Si]N-Sb(Cl)Me $\delta(^{19}F)$ = −76.95 ppm).[35] After removal of AgCl by filtration, concentration to incipient crystallization, and layering with *n*-hexane [TerP(NMe_2)$_2$]AuOTf (**3a**) and [TerP(NEt_2)$_2$]AuOTf (**3b**) were afforded as colourless solids in 64% and 49% isolated yield, respectively. X-Ray quality crystals of **3b** were obtained from a saturated CH_2Cl_2 solution layered with n-hexane after standing at 5°C for 24 h. **3b** crystallizes in the monoclinic spacegroup *C*2/*c* with 8 molecules in the unit cell (Figure 4, left). The Au–P distance is shorter than in **2a** and **2b** [(**3b**) P1–Au1 2.2187(4) Å], hinting at a more positive Au-center. This increase is further supported by two close contacts between gold and one of the flanking mesityl groups [C7–Au1 3.0506(14), C8–Au1 2.9955(13) Å]. Overall, the metrical parameters are close to complexes **2a** and **2b**.

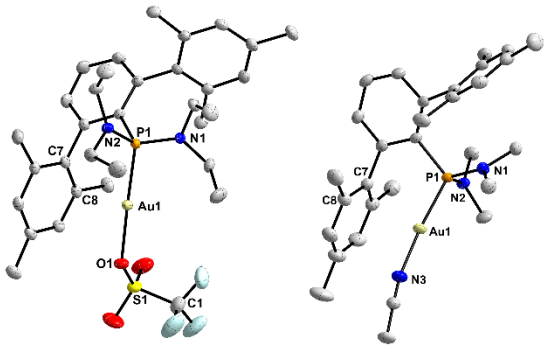

Figure 4. POV-Ray depiction of the molecular structure of **3b** (left) and **4a** (right). Ellipsoids are drawn at 50% probability, 150(2) K. All hydrogen atoms and the BF_4^- counter anion in **4a** have been omitted for clarity. Selected bond lengths (Å) and angles (°) of **3b** (left): C1–P1 1.8632(14), P1–N1 1.6528(13), P1–N2 1.6580(13), P1–Au1 2.2187(4), P1–O1 2.0948(11), C7–Au1 3.0506(14), C8–Au1 2.9955(13); N2–P1–N1 109.44(7), N1–P1–C1 115.66(6), N2–P1–C1 100.83(6), C25–N1–C26 115.42(13), C27–N1–P1 123.76(11), C25–N1–P1 120.55(11), C29–N2–C31 115.62(12), C29–N2–P1 124.48(10), C31–N2–P1 119.79(10), O1–Au1–P1 174.42(4). **4a** (right): P1–N2 1.6559(18), P1–N1 1.6588(19), P1–C1 1.837(2), P1–Au1 2.2376(5), Au1–N3 2.0431(18), C7–Au1 3.1364(23), C8–Au1 3.0504(24); N2–P1–N1 108.69(10), N2–P1–C1 101.34(9), N1–P1–C1 113.57(10); C25–N1–C26 112.75(18), C25–N1–P1 122.20(15), C26–N1–P1 123.72(15), C27–N2–C28 112.48(18), C27–N2–P1 117.44(15), C28–N2–P1 125.49(15), N3–Au1P1 174.33(6), C29–N3–Au1 169.5(2); Au1–P1–C1–C2 47.17(16).

To obtain an active catalyst for the hydroamination of alkynes with anilines, **2a** and **2b** were treated with $AgBF_4$ in CH_3CN and after filtration, an aliquot was taken for NMR analysis. In the ^{31}P NMR spectrum new signals highfield-shifted at 89.7 (**4a**) and 84.4 ppm (**4b**), respectively, compared to the starting material were detected. Broad resonances in the ^1H NMR spectrum at 0.98 and 1.46 ppm, respectively, indicate a coordinated CH_3CN molecule, which is further supported by a ^{19}F NMR shift for both complexes of −150.2 ppm, showing a non-interacting $[BF_4]^-$ anion. Colourless X-ray quality crystals of **4a** were obtained from a saturated C_6D_6 solution and revealed the expected ion-separated structure with a threefold disordered $[BF_4]^-$ anion (Figure 4, right). Additionally, we treated **2a** with $AgPF_6$ in CH_2Cl_2, added an excess of pyridine and the mixture was stirred overnight. Upon removal of the solvent and excess pyridine, X-Ray quality crystals were obtained from a saturated CH_2Cl_2 solution layered with *n*-hexane. In analogy to complex **4a** the base adduct, pyridine in this case, of the cationic gold complex was obtained with a non-coordinating $[PF_6]^-$ anion in [TerP(NMe_2)$_2$Au(py)][PF_6] (**5a**). In **4a** and **5a** the Au-P distances are similar to complexes **2** [P1–Au1 (**4a**) 2.2376(5); (**5a**) 2.247(3) Å; cf. (TerPMe_2)AuCl 2.2964(10) Å] and two contacts with the flanking mesityl group below 3.1 Å are detected in the base-stabilized cations. Overall, the structural parameters clearly show that the terphenyl structural motif gives rise to stabilizing Au-arene interactions, which should prove beneficial in catalytic trials, as was shown by Xu and co-workers in terms of complex stability in intermolecular hydroamination reactions.[15]

Preparing complexes **3**-**5**, sometimes the formation of a new species characterized by a doublet of doublets in the ^{31}P NMR spectrum was noted. This species was only observed if AgCl was not completely removed during filtration and when the solution was kept in daylight. In one instance we obtained X-ray quality crystals that were identified as the neutral silver chloride complex [(**1a**)AgCl]$_2$ (**6a**). We therefore conclude that it is of the utmost importance to carefully remove any traces of silver chloride and

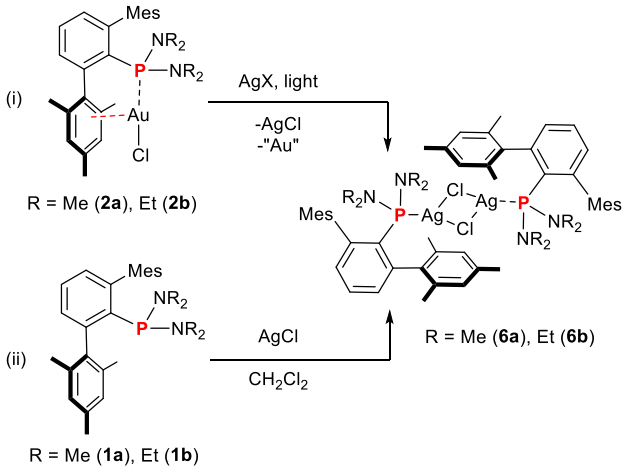

Scheme 3. Serendipitous decomposition of cationic gold complexes into [(**1**)AgCl]$_2$ dimeric complexes **6** (i) and their rational synthesis from L and AgCl (ii).

work in the dark, when preparing cationic gold complexes, as the formation of the respective ligand silver chloride complexes might proceed unnoticed and influence catalytic tests.[43] **6a** and the related complex [(**1b**)AgCl]$_2$ (**6b**) were independently synthesized by combining **1** with AgCl in a 1:1 stoichiometry in CH_2Cl_2 and continued stirring for 16 h under the exclusion of light afforded **6a** and **6b** as colourless air and moisture stable crystalline solids. In the ^{31}P NMR spectra **6a** and **6b** show two doublets due to coupling with the two spin ½ silver isotopes (^{107}Ag and ^{109}Ag) at 99.3 ($^1J_{109Ag,P}$ = 862.3 Hz, $^1J_{107Ag,P}$ = 746.4 Hz) and 94.3 ppm ($^1J_{109Ag,P}$ = 864.0 Hz, $^1J_{107Ag,P}$ = 748.9 Hz), respectively. X-ray quality crystals were grown from saturated acetone solutions in air. **6a** and **6b** (Figure 5) crystallize as centrosymmetric dimers in the monoclinic spacegroup $P2_1/c$ with two molecules in the unit cell, and in the orthorhombic spacegroup *Pbca* with four molecules in the unit cell, respectively.[33]

The molecular structures show a μ-Cl bridged dimer with a deltoid Ag_2Cl_2 core coordinated by two ligands **1a** or **1b**, respectively. The solid structures of **6a** and **6b** are closely related to that of [XPhosAg(μ-Cl)]$_2$ [(**6a**) P1−Ag1 2.3999(5), Ag1−Cl1 2.5060(6), Ag1−Cl1' 2.6120(6), Ag1−Ag1' 3.5277(5) Å, P1−Ag1−Cl1 130.064(19)°; (**6b**) P1−Ag1 2.4038(6) Å, Ag1−Cl1 2.5454(6) Å, Ag1−Cl1' 2.5657(6) Å, Ag1−Ag1' 3.6518(7) Å, P1−Ag1−Cl1 135.850(9)°; cf. [XPhosAg(μ-Cl)]$_2$ P1−Ag1 2.3941(6), Ag1−Cl1 2.4909(7), Ag1−Cl1' 2.6296(7), Ag1−Ag1' 3.393 Å].[44] Complexes with a (Ag-μ-Cl)2 core comprising a single phosphine ligand on Ag are rare and restricted to bulky monodentate phosphine ligands, such as P(NC$_4$H$_8$NMe)$_3$,[45] Ph$_2$P(CH$_2$)PPh$_2$C(H)C(O)C$_6$H$_4$Cl,[46] and the simple P*c*Hex$_3$.[47] To further characterize the electronic character of bisaminoterphenylphosphine ligands DFT calculations were carried out to determine the theoretical TEP-value (TEP$_{Ni,theo}$) of bisaminoterphenylphosphines **1**. Therefore, the complexes [(**1a**)·Ni(CO)$_3$] and [(**1b**)·Ni(CO)$_3$] were constructed *in silico* and their gas-phase structures were optimized at the BP86/def2SVP level of theory and confirmed as minima by frequency analyses.

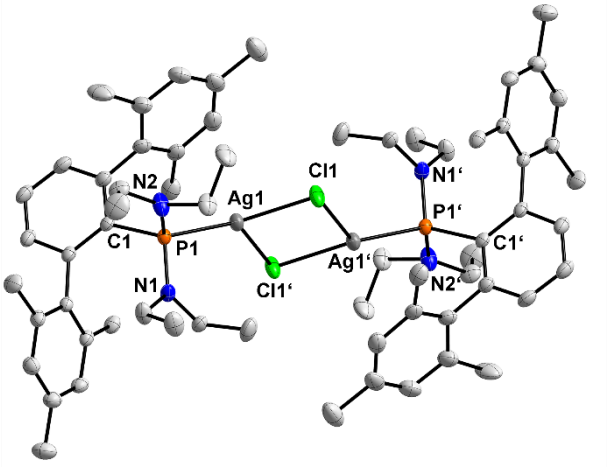

Figure 5. POV-Ray depiction of the molecular structure of **6b**. Ellipsoids are drawn at 30% probability, 150(2) K. All hydrogen atoms have been omitted for clarity. Selected bond lengths (Å) and angles (°): C1−P1 1.8652(18), P1−N1 1.6701(17), P1−N2 1.6700(17), P1−Ag1 2.4038(6), Ag1−Cl1 2.5060(6), Ag1−Cl1' 2.6120(6), Ag1−Ag1' 3.6518(7); P1−Ag1−Cl1 135.850(19), Ag1−Cl1−Ag1' 91.017(18).

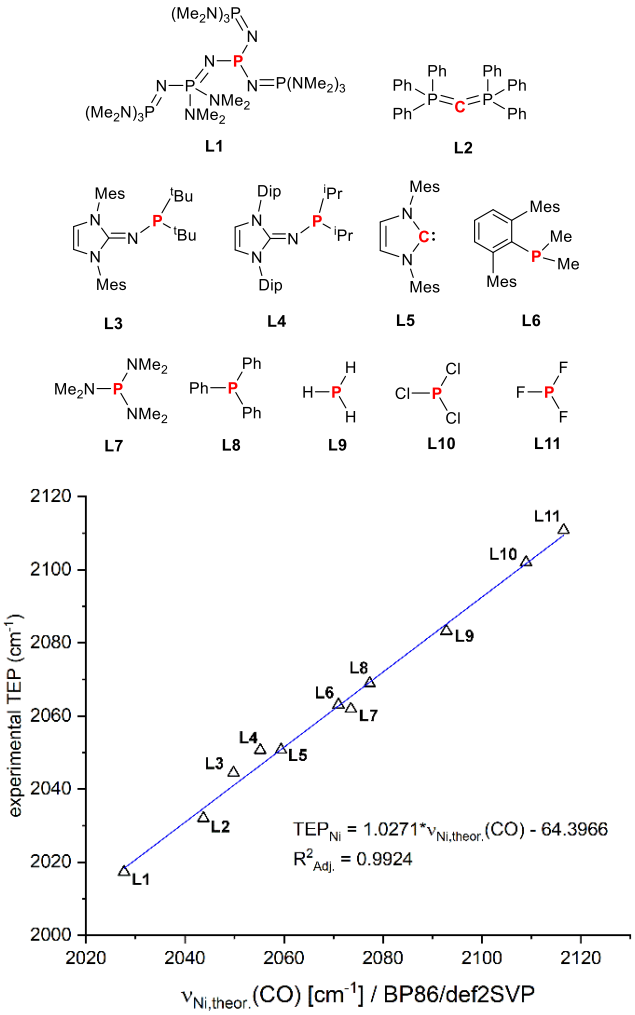

Figure 6. Diagram showing the correlation between experimental TEP_{Ni}-values of selected complexes $[LNi(CO)_3]$ and their corresponding theoretical $A_1(CO)$ values obtained at the BP86/def2SVP level of theory.

Of the resulting unscaled frequencies, the A_1 symmetrical CO stretching mode was chosen for the evaluation of the donor parameters. To fit the theoretical frequencies to experimental values, the $\upsilon_{theor.}(CO)$ for eleven different complexes $[LNi(CO)_3]$ were calculated and a linear dependency with respect to their experimental TEP values was noted (Figure 6).[33] Complexes were chosen to span from extremely electron-rich phosphazenyl phosphines to electron-poor phosphines such as PCl_3 and PF_3 giving a range of experimental TEPs from 2017.3 to 2110.8 cm^{-1}.[7, 8, 17, 18, 37, 48, 49] A linear regression allowed to derive the TEP_{Ni} values for ligands **1a** and **1b** of 2059.6 cm^{-1} and 2053.0 cm^{-1}, respectively. This is more electron rich than classical PPh_3 and approaches the donor strength of IMes, while the more electron rich IAPs and phosphazenyl phosphines are not surpassed. Especially **1b** is a stronger donor (based on TEP_{Ni}) than P^tBu_3 and falls in the range of newly developed YPhos ligands.[50] 2019 Carmona, Nicasio and co-workers described a series of nickel carbonyl complexes of dialkylterphenyl phosphines, and the A_1 mode for $[(TerPMe_2)Ni(CO)_3]$ was detected at 2063 cm^{-1}.[38] This illustrates the influence of the amino groups on phosphorus to render ligands **1a** and **1b** more electron rich and thus as a class with superior donor properties for the gold-catalyzed hydroamination of alkynes.

In order to evaluate the catalytic activity of complexes **4a** and **4b** in the hydroamination of aryl alkynes with anilines we first did a screening of the general reaction conditions, such as catalyst loading, solvent, temperature and reaction time using the phenylacetylene, *p*-toluidine pairing. Monitoring of the hydroamination between phenylacetylene and p-toluidine with 2 mol% of **4a** or **4b** in MeCN at 60°C showed that conversion plateaued after ca. 6 h. We therefore decided to run catalytic reactions overnight (ca. 16 h) to take into account different sterics of the substrates to be used. Variation of the catalyst loading revealed that no significant drop of conversion occurs going from 2 mol% to 1 mol% and minimally worse results were obtained with 0.5 mol%. Catalytic activity ceases when only 0.1 mol% of **4a** or **4b** were used as catalyst. Considering that in many gold-catalyzed transformations catalyst loadings in excess of 5 mol% are present,[9-11] this catalyst system is competitive with known systems. In a next series of experiments, we changed the solvent from MeCN to benzene and a minimal drop in conversion was noted. We

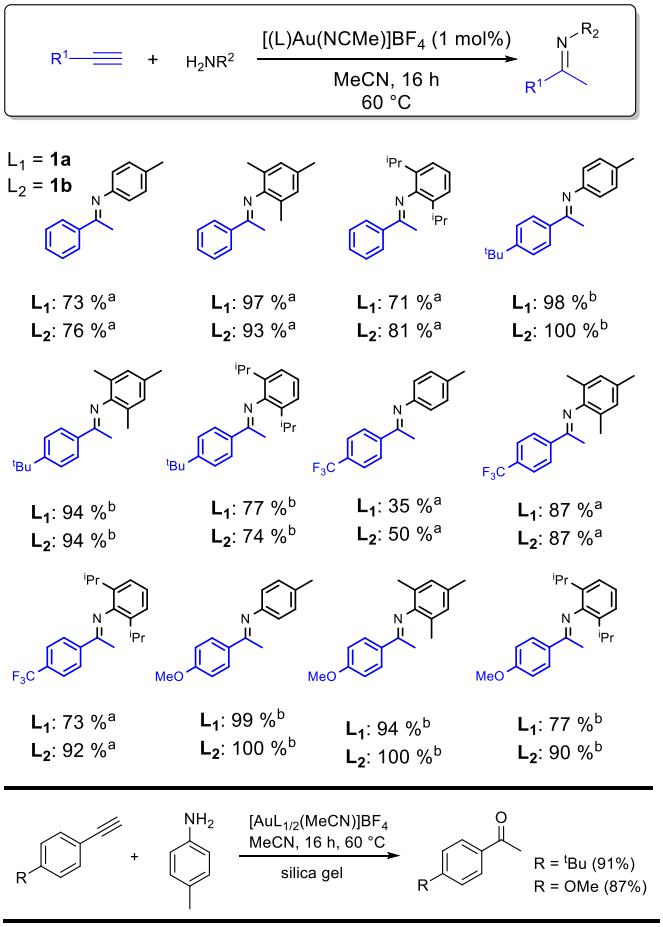

Scheme 3. Substrate scope of the gold-catalysed hydroamination of various aryl alkynes with anilines of varying bulk. ([a]denotes isolated yields; [b]denotes NMR yields, $(MeO)_3C_6H_3$ as internal standard)

Therefore, chose MeCN for our substrate scope. Lowering the temperature at optimized conditions from 60 °C to 40 °C resulted in a consistent drop of the isolated yield from 78% to 65%. We thus chose 60°C to evaluate the substrate scope.

With the optimized parameters in hand we tested both, different anilines and acetylenes (Scheme 3). To investigate the influence of the steric bulk of the aniline, p-toluidine, Mes-NH_2 (Mes = 2,4,6-$Me_3C_6H_2$) and Dip-NH_2 (Dip = 2,6-diisopropylphenyl) were tested. Overall, 12 different derivatives could be synthesized using different aryl-substituted alkynes. It should be noted that the electron-rich alkynes 4-MeO- and 4-^{t}Bu-phenylacetylene could be converted into the respective imines quantitively as determined by ^{1}H NMR spectroscopy, using 1,3,5-OMe_3-C_6H_3 as an internal standard. However, attempts to isolate these electron-rich imines after column chromatography on silica with $_n$-Hex/EtOAc (4:1) as the eluent, resulted in the isolation of the corresponding benzophenone derivatives in good isolated yields (Scheme 3, bottom). The isolated yields for the hydroamination of phenylacetylene are generally good, with up to 97% yield for the reaction with Mes-NH_2. Interestingly, for F_3C-C_6H_4-CCH with the yield increases with the steric demand of the respective aniline and up to 92% of the respective Dip-substituted imine were isolated. In general, we observed that the isolated yields are usually over 70% and nearly independent of whether **1a** or **1b** were used as a ligand. In summary, ligands of the type **1** represent a potent class of electron rich Buchwald-type phosphines, which have proven to be efficient in stabilizing Au(I) complexes for the intramolecular hydroamination of alkynes.

Conclusions

Overall, we report the isolation, spectroscopic and structural characterization of bulky bisaminoterphenyl phosphines **1**. These Buchwald-type ligands with flanking mesityl groups have been shown to possess attractive interactions between the gold center and one of the flanking mesityl groups, as was ascertained by determination of the molecular structures of a series of gold complexes **2**, **3**, **4** and **5**.The percent buried volume of **1b** amounts to ca. 55% and a linear fit of known TEP-values with their respective gas phase structures (obtained by DFT studies) revealed that particularly **1b** can be classified as electron-rich phosphine and their application in the intermolecular hydroamination of alkynes was tested. Preparing catalyst solutions by chloride ion abstraction from **2** with AgX salts, sometimes the formation of the respective dimeric Ag-complexes $[(L)Ag\text{-}\mu\text{-}Cl]_2$ **6a**

and **6b** was noted, which were independently synthesized. This is another example that AgCl contamination can result in erroneous catalyst screening results. Screening of the catalytic reaction conditions showed efficient hydroamination to take place at 60°C in MeCN with a catalyst loading of **4** of 1 mol% and moderate to excellent yields were achieved for bulky anilines such as Dip-NH_2 and different phenyl acetylene derivatives. No obvious difference in performance between ligands **1a** and **1b** was noted. In summary, terphenylbisaminophosphines meet the criteria of efficient ligands for intermolecular gold-catalyzed hydroamination reactions, as they combine strong donor properties with the 2-biphenyl structural motif, which is needed to enhance complex stability during catalysis.

Experimental

General methods

All reactions were performed under oxygen- and moisture-free conditions under an inert atmosphere of argon using standard Schlenk techniques or an inert atmosphere glovebox (MBraun LABstar ECO). Acetonitrile, diethylether, toluene, *n*-hexane and dichloromethane were purified with the Grubbs-type column system "Pure Solve MD-5" and dispensed into thick-walled Schlenk bombs equipped with Young-type Teflon valve stopcocks and stored under an atmosphere of argon prior to use. Benzene was refluxed over Na/benzophenone and freshly distilled prior to use. Dichloromethane was additionally refluxed over CaH_2 and freshly distilled prior to use Acetonitrile was additionally stored over molecular sieves (4 Å, 4-8 mesh) prior to use. C_6D_6 was refluxed over Na and freshly distilled prior to use. $CDCl_3$ was refluxed over P_4O_{10} and distilled prior to use. CD_2Cl_2 was refluxed over P_4O_{10} and distilled onto CaH_2 and was refluxed again and then distilled prior to use.
2,6-Mes_2-C_6H_3-I (Ter-I),[51] 2,6-Mes_2-C_6H_3-Li (Ter-Li),[52] and $ClP(NEt_2)_2$[53] have been reported previously and were prepared according to modified literature procedures. *n*-BuLi (2.5 M in n-hexane, ACROS), $ClP(NMe_2)_2$ (99%, Alfa Aesar), $AuCl(SMe_2)$ (>97%, TCI), $AgPF_6$ (98%, TCI), $AgSO_3CF_3$ (≥99%, Sigma Aldrich), AgCl (99 %, Sigma Aldrich) and $AgBF_4$ (98%, Sigma Aldrich) were stored under an argon atmosphere and used as received. $DippNH_2$ (ABCR, 90%) and $MesNH_2$ (98% Alfa Aesar) were distilled prior to use. Acetylenes PhCCH (98%, Sigma Aldrich), 4-OMe-C_6H_4-CCH (97 %, Sigma Aldrich), 4-CF_3-C_6H_4-CCH (97% Sigma Aldrich) and 4-^{t}Bu-C_6H_4-CCH (96%, Acros Organics) were recondensed, degassed three times and stored over sieves (4 Å) prior to use. Pyridine (99.8%, Sigma Aldrich) was refluxed over KOH, distilled and stored over molecular sieves (3 Å) prior to use.
^{1}H, ^{13}C{^{1}H}, ^{11}B, ^{19}F{^{1}H} and ^{31}P{^{1}H} NMR spectra were recorded on BRUKER AV300, AV400 or Fourier300 spectrometers. All ^{1}H NMR and ^{13}C NMR spectra are referenced using the chemical shifts of residual proton solvent resonances (benzene-d_6: δ_H 7.16, δ_C 128.06; chloroform-d: δ_H 7.26, δ_C 77.16; dichloromethane-d_2: δ_H 5.32, δ_C 53.84). Chemical shifts are reported in ppm (δ) relative to tetramethylsilane. The ^{31}P{^{1}H} NMR spectra were referenced to external 85% H_3PO_4 and the ^{19}F NMR spectra to $CFCl_3$ as external standard. IR spectra were recorded in ATR mode on a Bruker Alpha II IR spectrometer under an atmosphere of argon. Elemental analysis was done using a Leco Tru Spec elemental analyzer. Melting points were determined on a Mettler-Toledo MP 70 apparatus. Melting points are uncorrected and were measured in sealed capillaries under an Ar atmosphere. Mass spectra were recorded on a MAT 95XP Thermo Fisher mass spectrometer in electrospray ionization mode.

Synthesis of TerP(NMe_2)$_2$ (1a)

From Ter-Li: Terphenyllithium (0.994 g, 3.106 mmol) was suspended in toluene (80 mL) and the yellowish suspension was cooled to −78 °C. $ClP(NMe_2)_2$ (0.479 g, 3.106 mmol) in toluene (5 mL) was added dropwise over a period of 5 min. The cooling bath was removed, and the mixture was allowed to warm to ambient temperature over a period of 1 h. The resulting white suspension was filtered using a celite-padded frit. The filtrate was then concentrated to incipient crystallization (ca. 5 mL) and placed in the fridge (ca. 5 °C) for 72 h. This resulted in clear colorless blocks of TerP(NMe_2)$_2$ (**1a**, 0.898 g, 2.078 mmol, 67%). X-Ray quality crystals were obtained from a saturated n-hexane solution at 5°C after 24 h.
From Ter-I: Ter-I (2.500g, 5.677 mmol) was suspended in Et_2O and cooled to −78 °C and n-BuLi (2.49 mL, 2.5 M, 1.1 eq.) was added dropwise over a period of 5 min. The yellowish solution was allowed to warm to ambient temperatures over a period of 1 h and was then stirred for an additional 30 min. Subsequently, $ClP(NMe_2)_2$ (0.930 g, 6.016 mmol, 1.05 eq.) in Et_2O (10 mL) was added dropwise at −78 °C. The reaction mixture was slowly warmed to ambient temperature and stirred overnight. Afterwards, the solvent was removed under reduced pressure and the remaining white powder was extracted with toluene (65 mL) and filtered using a G4 frit, packed with celite. The volume of the clear filtrate was reduced to ca. 4 mL and the flask was placed in the freezer (−30 °C) for 48 h. This resulted in clear colorless blocks of TerP(NMe_2)$_2$ (**1a**, 1.940 g, 4.485 mmol, 79%).
^{1}H NMR (300 MHz, C_6D_6): δ = 7.12 (td, $^3J_{HH}$ = 7.2 Hz, $^5J_{HH}$ = 0.7 Hz, 1H, *p*-C_6H_3), 6.90 (dd, $^3J_{HH}$ = 7.2 Hz, $^4J_{PH}$ = 2.7 Hz, 2H, *m*-C_6H_3), 6.89 (s (br), 4H, *m*-C*H*-Mes), 2.24 (s, 6H, Ar-CH_3), 2.22 (s, 12H, Ar-CH_3), 2.21 (d, $^3J_{PH}$ = 8.6 Hz, 12H, NCH_3). **^{13}C{^{1}H} NMR** (75 MHz, $CDCl_3$): δ = 144.1, 140.5, 140.4, 135.6 (d, J_{CP} = 27.7 Hz), 130.5, 127.8, 127.7, 42.4 (d, $^2J_{CP}$ = 19.5 Hz), 21.4 (d, $^5J_{PC}$ = 5.0 Hz), 21.2. **^{31}P{^{1}H} NMR** (122 MHz, C_6D_6): δ = 103.42. **IR** (ATR, 32 scans, cm^{-1}): v = 2967 (w), 2915 (w), 2855 (m), 2827 (m), 2785 (m), 1608 (w), 1558 (w), 1478 (w), 1443 (m), 1375 (w), 1267 (m), 1197(m), 1059 (w), 979 (m), 964 (s), 848 (s), 809 (m), 773 (m), 755(m), 719 (w), 672 (s), 646 (m), 576 (m), 561 (m), 550 (m), 534 (w), 452 (m), 409 (m). **MS** (ESI-TOF): expected m/z = 433.2773, found: m/z = 433.2767. **EA**: calc.: C 77.74, H 8.62, N 6.48, found: C 77.39, H 8.54, N 6.08%.

Synthesis of TerP(NEt$_2$)$_2$ (1b)

From Ter-Li: Terphenyllithium (0.465 g, 1.428 mmol) was suspended in toluene (15 mL) and the yellowish suspension was cooled to −78°C. To this suspension ClP(NEt$_2$)$_2$ (0.360 g, 1.571 mmol) in toluene (5 mL) was added dropwise over a period of 5 min. The cooling bath was removed, and the mixture was allowed to warm to ambient temperature over a period of 1 h. Subsequently, toluene was removed using an external solvent trap, resulting in a yellowish pasty material, which was then extracted with n-hexane (20 mL) and filtered using a celite-padded frit (G4). The filtrate was then concentrated to incipient crystallization (ca. 2 mL) and placed in the fridge (ca. 5 °C) for 72 h. This resulted in colorless, X-ray quality blocks of TerP(NEt$_2$)$_2$ (**1b**, 0.273 g, 0.568 mmol, 40 %).

From Ter-I: Ter-I (2.500g, 5.677 mmol) was suspended in Et$_2$O and cooled to −78 °C and *n*-BuLi (2.49 mL, 2.5 M, 1.1 eq.) is added dropwise. The yellowish solution is allowed to warm to ambient temperatures over a period of 1 h and stirred for an additional 30 minutes. Then ClP(NEt$_2$)$_2$ (1.311 g, 6.245 mmol, 1.1 eq.) in Et$_2$O (10 mL) was added dropwise at −78 °C. The reaction mixture was slowly warmed to ambient temperature and was further stirred overnight. Afterwards the volatiles were evaporated, *n*-hexane (70 mL) was added to the solid yellow residue and the mixture was then filtered using a G4 frit packed with celite. The volume of the clear filtrate was reduced to ca. 4 mL and the flask was placed in the freezer (−30 °C) for 48 h. This resulted in the deposition of colorless, crystalline blocks, which were washed with 5 mL of cold *n*-hexane (−30 °C). TerP(NEt$_2$)$_2$ (**1b**, 2.472 g, 5.150 mmol, 89%).

^{1}H NMR (300 MHz, C_6D_6): δ = 7.10 (td, $^3J_{HH}$ = 7.1 Hz, $^5J_{HP}$ = 0.6 Hz, 1H, p-C_6H_3), 6.89 (d, ^{4}JHH = 0.7 Hz, 4H, m-Mes), 6.84 (dd, $^3J_{HH}$ = 7.1 Hz, $^4J_{PH}$ = 2.6 Hz, 2H, m-C_6H_3), 2.83-2.46 (m, 8H, NCH_2), 2.26 (s, 12H, Ar-CH_3), 2.24 (s, 6H, Ar-CH_3), 0.84 (t, $^3J_{HH}$ = 7.1 Hz, 12H, NCH$_2$CH_3). **^{13}C{1H} NMR** (75 MHz, C_6D_6): δ = 144.7 (d, JCP =18.38 Hz), 142.1 (d, J_{CP} =34.7 Hz), 141.2 (d, J_{CP} = 3.41 Hz), 136.2 (d, J_{CP} = 1.33 Hz), 135.7, 130.9, 128.6, 127.98, 45.8 (d, $^2J_{CP}$ = 20.4 Hz), 22.0 (d, $^5J_{CP}$ = 5.5 Hz), 21.2, 15.6 (d, $^3J_{CP}$ = 4.1 Hz). **^{31}P{1H} NMR** (122 MHz, C_6D_6): δ = 100.24. **IR** (ATR, 32 scans, cm-1): v = 2963 (m), 2913 (m), 2864 (m), 2835 (w), 2726 (w), 1610 (w), 1559 (w), 1443 (m), 1371(m), 1327 (w), 1293 (w), 1277 (w), 1189 (m), 1180 (s), 1117 (w), 1074 (w), 1026 (m), 1014 (s), 907 (m), 850 (s), 804 (m), 787 (m), 750 (m), 718 (w), 664 (m), 636 (m), 577 (w), 559 (w), 551 (w), 535 (w), 491 (w), 473 (m), 437 (m). **MS** (ESI-TOF): expected m/z = 489.3398, found: m/z = 489.3394. **EA**: calc.: C 78.65, H 9.28, N 5.73, found: C 78.49, H 9.10, N 5.51%.

Synthesis of TerP(NMe$_2$)$_2$AuCl (2a)

TerP(NMe$_2$)$_2$ (0.130 g, 0.30 mmol) and ClAu(SMe$_2$) (0.110 g, 0.30 mmol) were dissolved in dichloromethane (5 mL) under the exclusion of light (wrap flask with tin foil) and stirred at ambient temperature for 1 h. Subsequently, the volume of the reaction mixture was reduced to ca. 1 mL, layered with *n*-hexane (3-5 mL) and placed in the fridge (ca. 5 °C) for 72 h. This resulted in the deposition of colorless, X-ray quality crystals of [{TerP(NMe$_2$)$_2$}AuCl] (**2a**, 0.130 g, 0.20 mmol, 66 %).

^{1}H NMR (300 MHz, $CDCl_3$): δ = 7.51 (td, $^3J_{HH}$ = 7.1 Hz, $^5J_{HP}$ = 1.6 Hz, 1H, *p*-C_6H_3), 7.04 (dd, ^{3}JHH = 7.6 Hz, 4JPH = 4.0 Hz, 2H, m-C_6H_3), 6.89 (d, $^6J_{PH}$ = 0.7 Hz, 4H, *m*-Mes), 2.34 (s, 12H, Ar-CH_3), 2.31 (s, 6H, Ar-CH_3), 2.06 (s, 12H, NCH_3). **^{13}C NMR** (75 MHz, $CDCl_3$): δ = 145.8 (d, J_{CP} = 12.1 Hz), 138.5 (d, J_{CP} = 5.3 Hz), 137.2 , 135.6, 132.0 (d, $^3J_{CP}$ = 8.4 Hz), 131.4 (d, $^4J_{CP}$ = 2.0 Hz), 129.0, 41.2 (d, $^2J_{CP}$ = 9.1 Hz), 21.9, 21.2. **^{31}P{^{1}H} NMR** (122 MHz, $CDCl_3$): δ = 96.94. **MS** (ESI-TOF): expected m/z = 629.2360, found: m/z = 629.2368. **EA**: calc.: C 50.57, H 5.61, N 4.21, found: C 50.67, H 5.61, N 4.24%.

Synthesis of TerP(NEt$_2$)$_2$AuCl (2b)

TerP(NEt$_2$)$_2$ (0.960 g, 2.000 mmol) and ClAu(SMe$_2$) (0.600 g, 2.000 mmol) were dissolved in dichloromethane (20 mL) under the exclusion of light (wrap flask with tin foil) and stirred at ambient temperature for 1 h. The solvent was removed in vacuo, resulting in an off-white solid of TerP(NEt$_2$)$_2$AuCl (**2b**, 1.313 g, 1.821 mmol, 91 %). X-ray quality crystals were obtained from layering a saturated CH_2Cl_2 solution with *n*-hexane (5 °C for 72 h).

^{1}H NMR (300 MHz, C_6D_6): δ = 6.99 (t (br), $^3J_{HH}$ = 7.5, 1H, *p*-C_6H_3), 6.95 (m, 4H, *m*-Mes), 6.66 (dd, $^3J_{HH}$ = 7.5, $^4J_{PH}$ = 3.9 Hz, 2H, *m*-C_6H_3), 2.59 (q, $^3J_{HH}$ = 7.1 Hz, 4H, NCH_2), 2.56 (q, $^3J_{HH}$ = 7.1 Hz, 4H, NCH_2), 2.30 (s, 6H, Ar-CH_3), 2.09 (s, 12H, Ar-CH_3), 0.77 (t, $^3J_{HH}$ = 7.1 Hz, 12H, NCH$_2$CH_3). **^{13}C{^{1}H} NMR** (101 MHz, C_6D_6): δ = 146.1 (d, J_{CP} = 12.1 Hz), 139.6 (d, J_{CP} = 5.2 Hz), 137.4, 135.7, 134.3, 132.4 (d, J_{CP} = 8.0 Hz), 130.9 (d, J_{CP} = 2.1 Hz), 129.7, 44.7 (d, ^{3}JCP = 10.0 Hz), 22.4 , 21.3, 15.3 (d, $^4J_{CP}$ = 1.9 Hz). **^{31}P{^{1}H} NMR** (122 MHz, C_6D_6): δ = 93.26. **MS** (ESI-TOF): expected m/z = 743.2571, found: m/z = 743.2574. **EA**: calc.: C 53.30, H 6.29, N 3.88, found: C 53.26, H 6.25, N 3.64%. **MP** (° C): dec. >160 °C.

Synthesis of TerP(NMe$_2$)$_2$AuOTf (3a)

In a round-bottomed flask TerP(NMe$_2$)$_2$AuCl (66.5 mg, 0.100 mmol) and AgOTf (25.7 mg, 0.100 mmol) are suspended in 5 mL benzene under the exclusion of light. The solution was stirred at room temperature for 2 h and subsequently filtered using a filter canula. The volume of the filtrate was reduced to ca. 1 mL, layered with *n*-hexane (4 mL) and placed in the fridge (5 °C, 72 h). This resulted in the deposition of TerP(NMe)$_2$)$_2$AuOTf (50.1 mg, 0.064 mmol, 64 %) as an amorphous powder.

^{1}H NMR (300 MHz, C_6D_6): δ = 6.95 (td, $^3J_{HH}$ = 7.6 Hz, $^5J_{PH}$ = 1.7 Hz, 1H, *p*-C_6H_3), 6.91 – 6.82 (m, 4H, *m*-Mes), 6.62 (dd, $^3J_{HH}$ = 7.6 Hz, $^4J_{PH}$ = 4.3 Hz, 2H, *m*-C_6H_3), 2.28 (s, 6H, Ar-CH_3), 1.89 (s, 12H, Ar-CH_3), 1.84 (d, $^3J_{PH}$ = 11.3 Hz, 12H, NCH_3). **^{19}F{^{1}H} NMR** (282 MHz, C_6D_6): −76.8. **^{31}P{^{1}H} NMR** (122 MHz, C_6D_6): δ = 86.5.
X-Ray quality crystals of this compound could not be grown. CHN and MS were not obtained for this compound.

Synthesis of TerP(NEt$_2$)$_2$AuOTf (3b)

In a round-bottomed flask TerP(NEt$_2$)$_2$AuCl (0.100 g, 0.140 mmol) and AgOTf (0.036 mg, 0.140 mmol) are suspended in CH_2Cl_2 (5 mL) and the mixture stirred under the exclusion of light at room temperature for 1 h. Afterwards the mixture is filtered using a filter canula. The volume of the filtrate is reduced to ca. 1 mL, layered with n-hexane (4 mL) and placed in the fridge (5 °C, 72 h). This resulted in the deposition of colorless, X-ray quality crystals of TerP(NEt$_2$)$_2$AuOTf (0.054 g, 0.069 mmol, 49 %).
^{1}H NMR (300 MHz, C_6D_6): δ = 7.02-6.94 (m, 1H, *p*-C_6H_3), 6.92 (s, 4H, *m*-Mes), 6.62 (dd, 2H, *m*-C_6H_3), 2.63-2.44 (m, 8H, NCH_2), 2.31 (s, 6H, Ar-CH_3), 2.02 (s, 12H, Ar-CH_3), 0.76 (t, $^3J_{PH}$ = 7.1 Hz, 12H, NCH$_2$CH_3) ppm. **^{19}F{^{1}H} NMR** (376 MHz, CD_2Cl_2): δ = −76.62 ppm. **^{31}P{^{1}H} NMR** (162 MHz, CD_2Cl_2): δ = 78.89 ppm. **^{13}C{^{1}H} NMR** (75 MHz, CD_2Cl_2): δ = 146.28 (d, J_{CP} = 12.4 Hz), 139.18 (d, J_{CP} = 5.8 Hz), 138.13, 136.23, 133.12 (d, J_{CP} = 8.6 Hz), 132.25 (d, J_{CP} = 2.4 Hz), 129.5, 128.7, 44.5 (d, J = 9.6 Hz), 22.3, 21.3, 15.1. **MS** (ESI-TOF): expected m/z = 834.2506, found: m/z = TerP(NEt$_2$)$_2$Au 685.2980, AuOTf 345.1763. **EA**: calc.: C47.48, H5.43, N3.36, S3.84, found: C47.02, H5.69, N3.38, S3.89%.

Synthesis of [TerP(NMe$_2$)$_2$Au-MeCN]BF$_4$ (4a)

Complex **2a** (0.030 g, 0.045 mmol) and $AgBF_4$ (0.009 g, 0.045 mmol) combined in a round-bottomed flask, dissolved in acetontrile (2.5 mL) and stirred under exclusion of light for 30 min at room temperature. The solution was then filtered using a canula fitted with a glass microfiber filter. This mixture was then dried and extracted with benzene-d^6 and filtered into an NMR-tube equipped with a J-young-type screw cap. X-ray quality crystals of [TerP(NMe$_2$)$_2$Au-MeCN]BF_4 (**4a**) were obtained upon standing at room temperature for 48 h.
^{1}H NMR (300 MHz, C_6D_6): δ = 6.97 (td, $^3J_{HH}$ = 7.6 Hz, $^5J_{PH}$ = 1.7 Hz, 1H, *p*-C_6H_3), 6.88 (s, 4H, *m*-Mes), 6.62 (dd, $^3J_{HH}$ = 7.6 Hz, $^4J_{PH}$ = 4.2 Hz, 2H, *m*-C_6H_3), 2.27 (s, 6H, Ar-CH_3), 2.12 (d, $^3J_{PH}$ = 11.3 Hz, 12H, NMe_2), 1.93 (s, 12H, Ar-CH_3), 0.98 (s, 3H, CH_3CN). **^{19}F{^{1}H} NMR** (282 MHz, C_6D_6): −150.24 ppm. **^{31}P{^{1}H} NMR** (122 MHz, C_6D_6): δ = 89.7 ppm.
^{13}C NMR, CHN and MS were not obtained for this compound.

Synthesis of [TerP(NEt$_2$)$_2$Au-MeCN]BF$_4$ (4b)

Complex **2b** (0.032 g, 0.045 mmol) and $AgBF_4$ (0.009 g, 0.045 mmol) combined in a round-bottomed flask, dissolved in acetontrile (2.5 mL) and stirred under exclusion of light for 30 min at room temperature. The solution was then filtered using a canula fitted with a glass microfiber filter. This mixture was then dried and extracted with benzene-d^6 and filtered into an NMR-tube equipped with a J-young-type screw cap.
^{1}H NMR (300 MHz, C_6D_6): δ = 6.99 (td, $^3J_{HH}$ = 7.6 Hz, $^5J_{PH}$ = 1.7 Hz, 1H, p-C_6H_3), 6.94 (s, 4H, *m*-Mes), 6.60 (dd, $^3J_{HH}$ = 7.6 Hz, $^4J_{PH}$ = 4.0 Hz, 2H, *m*-C_6H_3), 2.67-2.52 (m, 8H, NCH_2CH$_3$) 2.41 (s, 6H, Ar-CH_3), 2.01 (s, 12H, Ar-CH_3), 1.46 (s, 3H, CH_3CN), 0.80 (t, $^3J_{HH}$ = 7.1 Hz, 12H, NCH$_2$CH_3). **^{19}F{^{1}H} NMR** (282 MHz, C_6D_6): −150.22 ppm. **^{31}P{^{1}H} NMR** (122 MHz, C_6D_6): δ = 84.4 ppm.
Single crystal X-ray analysis, ^{13}C NMR, CHN and MS were not obtained for this compound.

Synthesis of [TerP(NMe$_2$)$_2$Au-py]PF$_6$ (5a)

TerP(NMe$_2$)$_2$AuCl (0.066 g, 0.1 mmol) and $AgPF_6$ (0.025 g, 0.1 mmol) were dissolved in 5 mL dichloromethane. 10 µL pyridine was added to the solution and stirred overnight. After canula filtration the clear solution is reduced to 1 mL, layered with 5 mL hexane and placed in the freezer (−70 °C) for 4 h. The solvent was removed and the resulting colorless crystals of [TerP(NMe$_2$)$_2$Au-py]PF_6 (0.062 gg, 0.088 mmol, 88 %) were dried in vacuo.
^{1}H NMR (300 MHz,CD_2Cl_2): δ = 8.15-8.10 (m, 3H, p,m-C*H*-py), 7.73-7.68 (m, 2H, o-C*H*-py), 7.67-7.58 (m, 1H, *p*-C*H*-Ph), 7.09 (dd, $^1J_{HH}$ = 7.6 Hz, $^1J_{HP}$ = 4.2 Hz, 2H, *m*-C*H*-Ph), 6.88 (s, 4H, *m*-C*H*-Ph), 2.40 (s, 6H, NCH_3), 2.36 (s, 6H, NCH_3), 2.14 (s, 6H, Ar-CH_3), 2.07 (s, 6H, Ar-CH_3). **^{13}C NMR** (75 MHz, CD_2Cl_2): δ = 150.95 , 146.30 , 146.13 , 142.04 , 138.97 (d, $^2J_{CP}$ = 5.8 Hz), 137.78 , 136.82 , 132.76 (d, J_{CP} = 8.8 Hz), 129.26 , 127.10 , 40.81 (d, J_{CP} = 8.7 Hz), 22.00 , 21.15. **^{31}P NMR** (122 MHz, CD_2Cl_2): δ = 91.49, −144.45 (septet, $^1J_{P-F}$ = 707.6 Hz). **^{19}F NMR** (282 MHz, CD_2Cl_2): δ = −73.38 (d, J = 707.6 Hz).
Sufficient CHN analyses for this compound were not obtained, despite crystals showing no impurities on the basis of ^{1}H NMR spectroscopy.[33]

Synthesis of [TerP(NMe$_2$)$_2$AgCl]$_2$ (6a)

AgCl (0.019 g, 0.129 mmol) and TerP(NMe$_2$)$_2$ (0.056 g, 0.129 mmol) were dissolved in 5 mL of dichloromethane under the exclusion of light (wrap flask with tin foil) and the reaction mixture was stirred for 16 h at room temperature, which was

accompanied by precipitation of slight amounts of solid material. After canula filtration all volatile components were removed under vacuum, the residue was washed with small amounts of *n*-hexane (2×2 mL) and dried under vacuum to yield **6a** 0.046 g (0.040 mmol; 62%) as a colorless solid.
Crystals suitable for single-crystal X-ray diffraction were obtained by slow evaporation of a solution of **6a** in acetone.
^{1}H NMR (300 MHz, $CDCl_3$, 298 K): d = 7.47-7.51 (m, 2H, *p*-$CH_{Aryl}P$), 7.00-7.03 (m, 4H, *m*-$CH_{Aryl}P$), 6.99-7.00 (m, 8H, CH_{Mes}), 2.34 (s, 12H, Ar-C*H*$_3$), 2.28 (s, 12H, N(C*H*$_3$)$_2$), 2.25 (s, 12H, N(C*H*$_3$)$_2$), 2.04 (s, 24H, Ar-C*H*$_3$), ppm. **^{13}C{^{1}H} NMR** (75 MHz, $CDCl_3$, 298 K): d = 21.2 (*p*-$\underline{C}H_3C_6H_3$), 21.55 (*o*-$\underline{C}H_3C_6H_3$), 21.57 (*o*-$\underline{C}H_3C_6H_3$), 41.78 (d, $^{2}J_{P,C}$ = 13.5 Hz, $N(CH_3)_2$), 41.80 (d, $^{2}J_{P,C}$ = 13.7 Hz, $N(CH_3)_2$), 129.2 (CH_{Mes}), 130.9 (*p*-$CH_{Aryl}P$), 131.4 (d, $^{3}J_{P,C}$ = 5.8 Hz, *m*-$CH_{Aryl}P$), 133.7 (m, $C_{q,Aryl}P$), 135.2 (*o*-$\underline{C}_{q,Mes}C_6H_3$), 137.4 (*p*-$\underline{C}_{q,Mes}C_6H_3$), 138.0 (d, $^{3}J_{P,C}$ = 6.1 Hz, $C_{q,Mes}$), 144.5 (d, $^{2}J_{C,P}$ = 15.3 Hz, *o*-$C_{q,Aryl}P$) ppm. **^{31}P{^{1}H} NMR** (122 MHz, $CDCl_3$, 298 K): d = 99.3 (dd, $^{1}J_{Ag,P}$ = 862.3 Hz, $^{1}J_{Ag,P}$ = 746.4 Hz) ppm. **MS** (ESI-TOF): expected: m/z = 1113.3184 [M-Cl]+; found: m/z = 1113.3202. **EA**: calculated: C 58.40, H 6.48, N 4.86; found: C 58.56, H 6.96, N 4.34%.

Synthesis of $[TerP(NEt_2)_2AgCl]_2$ (6b)

AgCl (0.147 g, 1.023 mmol) and $TerP(NEt_2)_2$ (0.500 g, 1.023 mmol) were dissolved in 15 mL of dichloromethane under the exclusion of light (wrap flask with tin foil) and the reaction mixture was stirred for 16 h at room temperature which was accompanied by precipitation of slight amounts of solid material. After canula filtration all volatile components were removed under vacuum, the residue was washed with *n*-hexane (2×5 mL) and dried under vacuum to yield **6b** 0.546 g (0.422 mmol; 83%) as a colorless solid. Crystals suitable for single-crystal X-ray diffraction were obtained by slow evaporation of a solution of **6b** in acetone.
^{1}H NMR (300 MHz, $CDCl_3$, 298 K): d = 0.91 (t, $^{3}J_{H,H}$ = 7.1 Hz, 24H, NCH_2CH_3), 2.10 (s, 24H, *o*-C*H*$_3$C$_6$H$_3$), 2.36 (s, 12H, *p*-C*H*$_3$C$_6$H$_3$), 2.54-2.79 (m, 16H, NC*H*$_2$CH$_3$), 6.94-6.97 (m, 4H, *m*-$CH_{Aryl}P$), 7.00-7.01 (m, 8H, CH_{Mes}), 7.44-7.48 (m, 2H, *p*-$CH_{Aryl}P$) ppm. **^{13}C{^{1}H} NMR** (75 MHz, $CDCl_3$, 298 K): d = 15.1 (d, $^{3}J_{P,C}$ = 2.7 Hz, $NCH_2\underline{C}H_3$) 21.3 (*p*-$\underline{C}H_3C_6H_3$), 21.83 (*o*-$\underline{C}H_3C_6H_3$), 21.84 (*o*-$\underline{C}H_3C_6H_3$), 45.0 (d, $^{2}J_{P,C}$ = 17.0 Hz, $N\underline{C}H_2CH_3$), 129.6 (CH_{Mes}), 130.6 (*p*-$CH_{Aryl}P$), 131.8 (d, $^{3}J_{P,C}$ = 5.5 Hz, *m*-$CH_{Aryl}P$), 133.9 (m, $C_{q,Aryl}P$), 135.2 (*o*-$\underline{C}_{q,Mes}C_6H_3$), 137.7 (*p*-$\underline{C}_{q,Mes}C_6H_3$), 138.8 (d, $^{3}J_{P,C}$ = 6.3 Hz, $C_{q,Mes}$), 144.5 (m, *o*-$C_{q,Aryl}P$) ppm. **^{31}P{^{1}H} NMR** (122 MHz, $CDCl_3$, 298 K): d = 94.3 (dd, $^{1}J_{Ag,P}$ = 864.0 Hz, $^{1}J_{Ag,P}$ = 748.9 Hz) ppm. **MS** (ESI-TOF): expected: m/z = 1227.4428 [M-Cl]+; found: m/z = 1227.4449. **EA**: calculated: C 60.81, H 7.18, N 4.43; found: C 60.83, H 7.74, N 4.28%.

Catalytic hydroamination of acetylenes.

The complex [Au(L)Cl] (0.045 mmol, 1 equiv; L = 1a, 1b) and AgBF4 (0.045 mmol, 1 equiv) were dissolved in MeCN (2.5 mL) and stirred under exclusion of light for 30 min at room temperature and the solution was then filtered using a filter canula fitted with a glass microfiber filter. This 0.018 M solution was used as a stock solution. Acetylenes (0.455 mmol) and aryl amines (0.503 mmol) were weighed in a glovebox and were dissolved in 1.75 mL MeCN in a vial fitted with a septum screw cap. Afterwards 0.25 mL of the respective catalyst standard solutions of was added and stirred for 16 h at 60 °C. The NMR yields were determined by ^{1}H NMR spectroscopy as an average of two runs using 1,3,5-MeO-C_6H_3 as an internal standard. The characteristic singlet of the CH^3 group of the imines that appears around 2.3 ppm was used for the integration. For the isolated yields, the products were purified by column chromatography on silica gel. Spectroscopic data is provided in the ESI.[33]

Conflicts of interest

There are no conflicts to declare.

Acknowledgements

C. H.-J. thanks Prof. M. Beller for his support, the European Union for funding (H2020-MSCA-IF-2017 792177), the Max Buchner-Foundation for a Scientific Fellowship and support by an Exploration Grant of the Boehringer Ingelheim Foundation (BIS) is acknowledged. We thank our technical and analytical staff for assistance, especially Dr. Anke Spannenberg for her support regarding X-ray analysis. Dr. Alexander Villinger is acknowledged for assistance with the X-ray analysis of **4a**. Dr. Jonas Bresien is kindly acknowledged for help with vibrational spectroscopy and fruitful discussions on DFT calculations.

Notes and references

1. B. F. Straub, *Angew. Chem. Int. Ed.*, 2010, **49**, 7622-7622.
2. D. W. Old, J. P. Wolfe and S. L. Buchwald, *J. Am. Chem. Soc.*, 1998, **120**, 9722-9723.
3. B. P. Fors, D. A. Watson, M. R. Biscoe and S. L. Buchwald, *J. Am. Chem. Soc.*, 2008, **130**, 13552-13554.
4. T. Ikawa, T. E. Barder, M. R. Biscoe and S. L. Buchwald, *J. Am. Chem. Soc.*, 2007, **129**, 13001-13007.

5. T. E. Barder, S. D. Walker, J. R. Martinelli and S. L. Buchwald, *J. Am. Chem. Soc.*, 2005, **127**, 4685-4696.
6. D. S. Surry and S. L. Buchwald, *Angew. Chem. Int. Ed.*, 2008, **47**, 6338-6361.
7. C. A. Tolman, *J. Am. Chem. Soc.*, 1970, **92**, 2956-2965.
8. C. A. Tolman, *Chem. Rev.*, 1977, **77**, 313-348.
9. A. S. K. Hashmi, *Chem. Rev.*, 2007, **107**, 3180-3211.
10. A. Arcadi, *Chem. Rev.*, 2008, **108**, 3266-3325.
11. Z. Li, C. Brouwer and C. He, *Chem. Rev.*, 2008, **108**, 3239-3265.
12. R. H. Hertwig, W. Koch, D. Schröder, H. Schwarz, J. Hrušák and P. Schwerdtfeger, *J. Phys. Chem.*, 1996, **100**, 12253-12260.
13. D. J. Gorin and F. D. Toste, *Nature*, 2007, **446**, 395-403.
14. A. S. K. Hashmi, *Angew. Chem. Int. Ed.*, 2010, **49**, 5232-5241.
15. W. Wang, G. B. Hammond and B. Xu, *J. Am. Chem. Soc.*, 2012, **134**, 5697-5705.
16. D. G. Gusev, *Organometallics*, 2009, **28**, 6458-6461.
17. T. Witteler, H. Darmandeh, P. Mehlmann and F. Dielmann, *Organometallics*, 2018, **37**, 3064-3072.
18. S. Ullrich, B. Kovačević, X. Xie and J. Sundermeyer, *Angew. Chem. Int. Ed.*, 2019, **58**, 10335-10339.
19. J. A. C. Clyburne and N. McMullen, *Coord. Chem.Rev.*, 2000, **210**, 73-99.
20. T. Nguyen, A. D. Sutton, M. Brynda, J. C. Fettinger, G. J. Long and P. P. Power, *Science*, 2005, **310**, 844.
21. E. Rivard and P. P. Power, *Inorg. Chem.*, 2007, **46**, 10047-10064.
22. R. C. Fischer and P. P. Power, *Chem. Rev.*, 2010, **110**, 3877-3923.
23. D. L. Kays, *Chem.l Soc. Rev.*, 2016, **45**, 1004-1018.
24. K. Ruhlandt-Senge, J. Ellison, R. Wehmschulte, F. Pauer and P. Power, *J. Am. Chem. Soc.*, 1993, **115**, 11353-11357.
25. C. Gerdes, W. Saak, D. Haase and T. Müller, *J. Am. Chem. Soc.*, 2013, **135**, 10353-10361.
26. A. J. Veinot, A. D. K. Todd and J. D. Masuda, *Angew. Chem. Int. Ed.*, 2017, **56**, 11615-11619.
27. E. Urnéžius and J. D. Protasiewicz, *Main Group Chem.*, 1996, **1**, 369-372.
28. C. M. E. Graham, T. E. Pritchard, P. D. Boyle, J. Valjus, H. M. Tuononen and P. J. Ragogna, *Angew. Chem. Int. Ed.*, 2017, **56**, 6236-6240.
29. D. V. Partyka, M. P. Washington, J. B. Updegraff, X. Chen, C. D. Incarvito, A. L. Rheingold and J. D. Protasiewicz, *J. Organomet. Chem.*, 2009, **694**, 1441-1446.
30. A. Orthaber, F. Belaj, J. H. Albering and R. Pietschnig, *Eur. J. Inorg. Chem.*, 2010, **2010**, 34-37.
31. R. C. Smith, R. A. Woloszynek, W. Chen, T. Ren and J. D. Protasiewicz, *Tetrahedron Lett.*, 2004, **45**, 8327-8330.
32. B. Buster, A. A. Diaz, T. Graham, R. Khan, M. A. Khan, D. R. Powell and R. J. Wehmschulte, *Inorganica Chim. Acta*, 2009, **362**, 3465-3474.
33. *See ESI for more information*. CIFs available from the CCDC, deposition numbers 2014543-2014551.
34. P. Pyykkö and M. Atsumi, *Chem. –Eur. J.*, 2009, **15**, 12770-12779.
35. C. Hering, M. Lehmann, A. Schulz and A. Villinger, *Inorg. Chem.*, 2012, **51**, 8212-8224.
36. E. Deck, H. E. Wagner, J. Paradies and F. Breher, *Chem. Commun.*, 2019, **55**, 5323-5326.
37. M. Marín, J. J. Moreno, M. M. Alcaide, E. Álvarez, J. López-Serrano, J. Campos, M. C. Nicasio and E. Carmona, *J. Organomet. Chem.*, 2019, **896**, 120-128.
38. M. Marín, J. J. Moreno, C. Navarro-Gilabert, E. Álvarez, C. Maya, R. Peloso, M. C. Nicasio and E. Carmona, *Chem. – Eur. J.*, 2019, **25**, 260-272.
39. R. F. W. Bader, *Acc. Chem. Res.*, 1985, **18**, 9-15.
40. S. Shahbazian, *Chem. –Eur. J.*, 2018, **24**, 5401-5405.
41. L. Falivene, R. Credendino, A. Poater, A. Petta, L. Serra, R. Oliva, V. Scarano and L. Cavallo, *Organometallics*, 2016, **35**, 2286-2293.
42. H. Clavier and S. P. Nolan, *Chem. Commun.*, 2010, **46**, 841-861.
43. A. Homs, I. Escofet and A. M. Echavarren, *Org. Lett.*, 2013, **15**, 5782-5785.
44. A. Grirrane, E. Álvarez, H. García and A. Corma, *Chem. – Eur. J.*, 2016, **22**, 340-354.
45. C. Ganesamoorthy, J. T. Mague and M. S. Balakrishna, *Eur. J. Inorg. Chem.*, 2008, **2008**, 596-604.
46. S. J. Sabounchei, M. Pourshahbaz, S. Salehzadeh, M. Bayat, R. Karamian, M. Asadbegy and H. R. Khavasi, *Polyhedron*, 2015, **85**, 652-664.
47. G. A. Bowmaker, Effendy, P. J. Harvey, P. C. Healy, B. W. Skelton and A. H. White, *J. Chem. Soc., Dalton Trans.*, 1996, , 2459-2465.
48. W. Petz, F. Weller, J. Uddin and G. Frenking, *Organometallics*, 1999, **18**, 619-626.
49. R. Dorta, E. D. Stevens, N. M. Scott, C. Costabile, L. Cavallo, C. D. Hoff and S. P. Nolan, *J. Am. Chem. Soc.*, 2005, **127**, 2485-2495.
50. T. Scherpf, C. Schwarz, L. T. Scharf, J.-A. Zur, A. Helbig and V. H. Gessner, *Angew. Chem. Int. Ed.*, 2018, **57**, 12859-12864.
51. F. Reiß, A. Schulz, A. Villinger and N. Weding, *Dalton Trans.*, 2010, **39**, 9962-9972.
52. K. Ruhlandt-Senge, J. J. Ellison, R. J. Wehmschulte, F. Pauer and P. P. Power, *J. Am. Chem. Soc.*, 1993, **115**, 11353-11357.
53. P. Wucher, J. B. Schwaderer and S. Mecking, *ACS Catalysis*, 2014, **4**, 2672-2679.